PAPER

Solution-processed indacenodithiophene-based small molecule for bulk heterojunction solar cells

Weina Yong,[ab] Maojie Zhang,*[b] Xiaodong Xin,[b] Zhaojun Li,[b] Yue Wu,[b] Xia Guo,[b] Zhou Yang*[a] and Jianhui Hou*[b]

A novel small molecule with a acceptor–donor–acceptor (A–D–A) structure, IDT(BTTh$_2$)$_2$, containing an electron-rich indacenodithiophene (IDT) unit as core, flanked by electron-deficient 2,1,3-benzothiadiazole (BT) units and end-capped with hexyl-substituted bithiophene units, has been synthesized for photovoltaic application. IDT(BTTh$_2$)$_2$ shows a broad absorption in the visible range with an optical band gap of *ca.* 1.80 eV and possesses a relatively deep HOMO level at −5.21 eV. The solution-processed bulk heterojunction solar cells based on the blend of IDT(BTTh$_2$)$_2$/PC$_{71}$BM (1 : 3, w/w) without using any treatment such as a solvent additive or thermal annealing, showed a power conversion efficiency (PCE) of 4.25% with a high open-circuit voltage (V_{oc}) of 0.93 V, a short-circuit current (J_{sc}) of 9.42 mA cm^{-2} and a fill factor (FF) of 48.5%, under the illumination of AM 1.5G at 100 mW cm^{-2}. These results indicate that indacenodithiophene-based small molecules are promising for bulk heterojunction solar cells.

Introduction

In the past few years, small-molecule bulk-heterojunction (SM BHJ) solar cells have attracted considerable research interest owing to their well-defined molecular weight and structure, easier purification and scale-up, and lower batch-to-batch variation, as compared to the polymer-based organic photovoltaic cells (OPVs).[1–3] Recently, the dramatic improvement in photovoltaic performance of the SM BHJ solar cells has been achieved with power conversion efficiencies (PCEs) up to 6–8%.[4–14] However, the overall performances of SM BHJs are still lower than those of their polymer counterparts.[15–21] From the point of view of the molecular design of small molecular donor materials, good solubility, a narrower band gap with broad absorption, a relatively lower HOMO (the highest occupied molecular orbital) energy level and higher hole mobility are key issues for high photovoltaic performance.[7–11] So far, one of the most successful small molecular structures to satisfy these requirements is the acceptor–donor–acceptor (A–D–A) structure with a conjugated planar electron-rich unit as the core and an electron-deficient unit as the acceptor.[22–26] For example, the small molecule DTS(PTTh$_2$)$_2$[9] consisting of dithieno[3,2-*b*;2′,3′-*d*]silole (DTS) as core and the [1,2,5]thiadiazolo[3,4-*c*]pyridine (PT) unit as acceptor exhibited a broad absorption with a narrow optical band gap of 1.5 eV and a low-lying HOMO energy level of −5.2 eV resulting from intra-molecular charge transfer, and the high mobility of 0.1 cm^2 V^{-1} s^{-1} beneficial from the planar structure and efficient π–π interaction. Hence, the SM BHJ solar cells based on DTS(PTTh$_2$)$_2$ showed a power conversion efficiency (PCE) of 6.7% with an open-circuit voltage (V_{oc}) of 0.78 V, a short-circuit current (J_{sc}) of 14.4 mA cm^{-2} and a fill factor (FF) of 59.3%.

Recently, the indacenodithiophene (IDT) unit has attracted great interest as a donor building block for conjugated polymers for photovoltaic application due to its large and rigid planar conjugated structure, which can enhance the π electron delocalization and promote intermolecular π–π interaction, thus beneficial for charge transport in devices.[27–36] To date, conjugated polymers based on IDT unit have led to the achievement of PCEs over 7%.[37] However, to the best of our knowledge, small molecules based on the IDT unit as a building block have not been reported.

In this work, we synthesized a novel small molecule with A–D–A structure, IDT(BTTh$_2$)$_2$ (as shown as in Scheme 1), consisting of IDT unit as core flanked by benzo[*c*][2,1,3]-thiadiazole unit and terminated with hexyl-substituted bithiophene. This small molecule exhibits broad absorption in visible range and a low-lying HOMO energy level of −5.21 eV. The solution-processed bulk heterojunction solar cells based on the blend of IDT(BTTh$_2$)$_2$/PC$_{71}$BM (1 : 3 w/w) showed a PCE of 4.25% with a high V_{oc} of 0.93 V, a J_{sc} of 9.42 mA cm^{-2} and a FF of 48.5%, under the illumination of AM 1.5G at 100 mW cm^{-2}.

[a]Department of Materials Physics and Chemistry, School of Materials Science and Engineering, University of Science and Technology Beijing, Beijing, 100083, China. E-mail: yangz@ustb.edu.cn

[b]State Key Laboratory of Polymer Physics and Chemistry, Beijing National Laboratory for Molecular Sciences Institute of Chemistry, Chinese Academy of Sciences, Beijing 100190, China. E-mail: hjhzlz@iccas.ac.cn; zmj2008@iccas.ac.cn
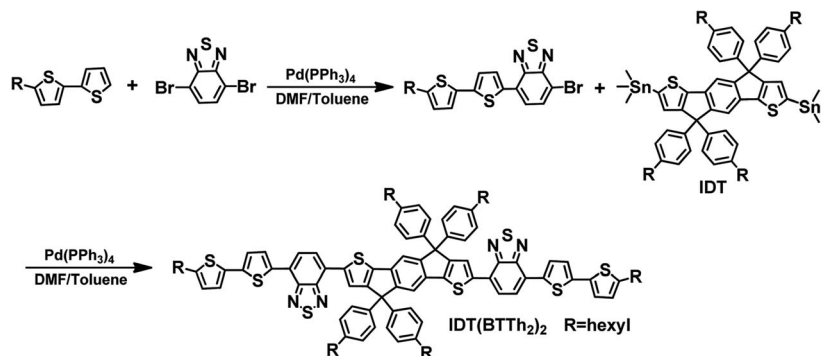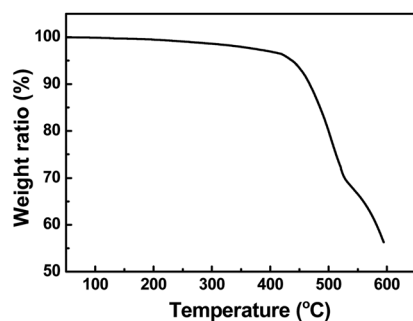
Scheme 1 Synthetic route of IDT(BTTh$_2$)$_2$.

Fig. 1 TGA plot of IDT(BTTh$_2$)$_2$ with a heating rate of 10 °C min^{-1} under air atmosphere.
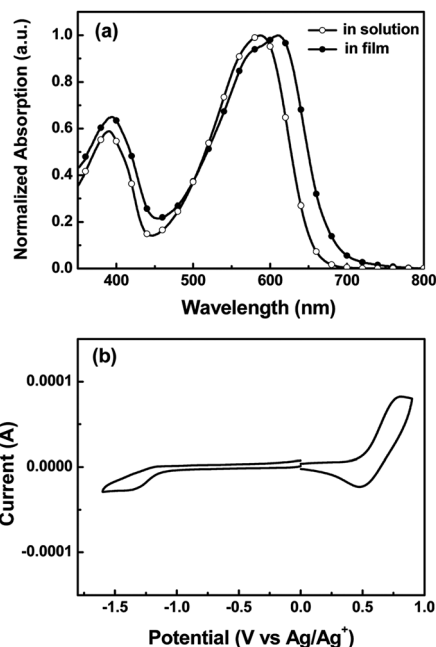

Fig. 2 (a) Absorption spectra of IDT(BTTh$_2$)$_2$ in o-DCB solution and in film. (b) Cyclic voltammogram of IDT(BTTh$_2$)$_2$ films on a glassy carbon disk measured in 0.1 mol L^{-1} Bu$_4$NPF$_6$ acetonitrile solutions at a scan rate of 50 mV s^{-1}.

Experimental

Materials

4,7-Dibromobenzo[c][2,1,3]thiadiazole was purchased from Solarmer Materials Inc.; [Pd(PPh$_3$)$_4$] was purchased from Frontiers Scientific Inc. All of these chemicals were used as received. Tetrahydrofuran (THF) was dried over Na/benzophenone ketyl and freshly distilled prior to use. The other materials were of the common commercial level and used as received. The molecular structure and synthetic routes are shown in Scheme 1.

Measurements and characterization

All new compounds were characterized by ^{1}H NMR spectroscopy performed on a Bruker DMX-400 spectrometer. For the ^{1}H-NMR measurements, CDCl$_3$ was used as the solvent. Chemical shifts in the NMR spectra were reported in ppm relative to the singlet at 7.26 ppm for CDCl$_3$. Thermogravimetric analysis (TGA) was performed using a PE Inc., Pyris 1 thermogravimetric analyzer. UV-Vis absorption spectra were obtained using a Hitachi U-3010 spectrometer. Cyclic voltammetry (CV) was performed using a Zahner IM6e Electrochemical Workstation with a three-electrode system in a solution of 0.1 M Bu$_4$NPF$_6$ in acetonitrile at a scan rate of 50 mV s^{-1}. The IDT(BTTh$_2$)$_2$ films were coated on a glassy carbon disk by dipping the electrode into the corresponding solutions and then drying. A Pt wire was used as the counter electrode, and Ag/Ag$^+$ was used as the reference electrode. AFM measurements were performed using a Bruker Ceeco MultiMode 8 Atomic Force Microscope, and TEM measurements were performed using a Transmission Electron Microscope (TEM): JEM-2200FS.

Fabrication and characterization of organic solar cells

Organic solar cells (OSCs) were fabricated with ITO glass as a positive electrode, Ca/Al as a negative electrode and the blend film of the IDT(BTTh$_2$)$_2$/PC$_{71}$BM between them as a photosensitive layer. The ITO glass was precleaned and modified using a thin layer of PEDOT:PSS which was spin-cast from a PEDOT:PSS aqueous solution (Clevios™ P VP AI 4083, H.C. Stark, Germany) on the ITO substrate, and the thickness of the PEDOT:PSS layer is about 30 nm. The photosensitive layer was prepared by spin-coating a blend solution of IDT(BTTh$_2$)$_2$ and
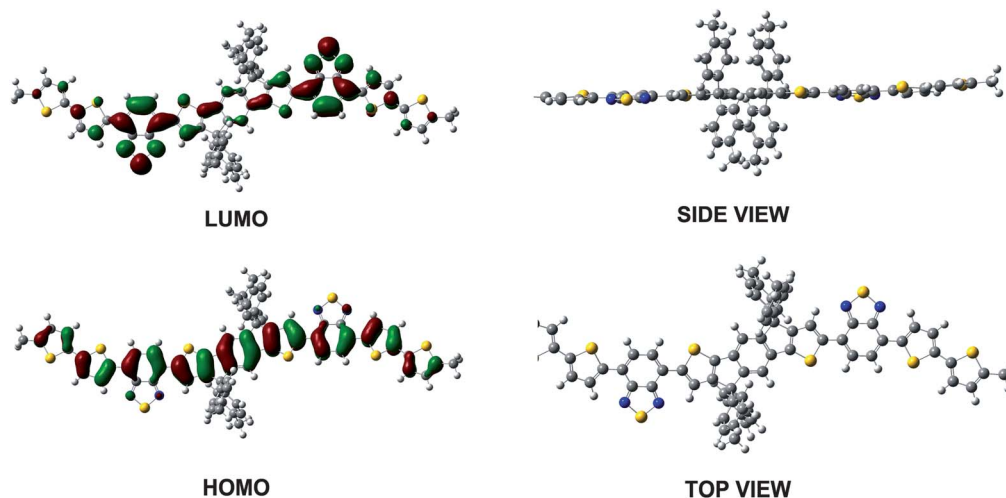
Fig. 3 The optimized molecular geometry, LUMO and HOMO orbital surfaces for IDT(BTTh₂)₂ calculated by DFT/B3LYP/6-31G(d,p) level.

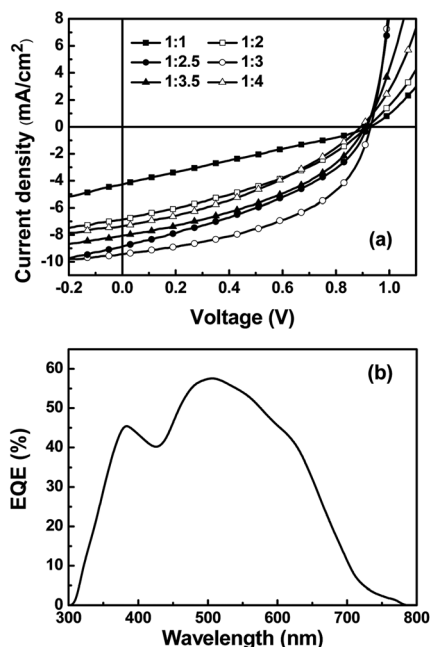**Fig. 4** (a) J–V curves of the SM BHJ solar cells based on IDT(BTTh₂)₂:PC₇₁BM under the illumination of AM 1.5G at 100 mW cm⁻². (b) EQE curve of the devices based on IDT(BTTh₂)₂:PC₇₁BM (1 : 3, w/w).

Table 1 Photovoltaic performances of the devices based on IDT(BTTh₂)₂:PC₇₁BM with different weight ratios

IDT(BTTh₂)₂:PC₇₁BM (wt/wt)	V_{oc} (V)	J_{sc} (mA cm⁻²)	FF (%)	PCE (%)
1 : 1	0.93	4.28	26.4	1.05
1 : 2	0.92	6.86	36.3	2.27
1 : 2.5	0.92	8.86	38.5	3.13
1 : 3	0.93	9.42	48.5	4.25
1 : 3.5	0.91	8.05	40.5	2.97
1 : 4	0.89	7.34	36.2	2.37

PC₇₁BM ([6,6]-phenyl C₇₁ butyric acid methyl ester) in *ortho*-dichlorobenzene (*o*-DCB) on the ITO/PEDOT:PSS electrode. In the case of the devices using a processing additive, 1,8-diiodooctane (1%, 2% or 3% by volume) was added to the solutions before use. For the thermal annealing case, the blend solution of IDT(BTTh₂)₂/PC₇₁BM in *o*-DCB (1 : 3 w/w) was spin-coated on top of the PEDOT:PSS layer and then annealed at 110 °C, 130 °C or 150 °C for 10 min in a glovebox. Then the Ca/Al cathode was deposited on the photosensitive layer by vacuum evaporation under 3 × 10⁻⁵ Pa. The thickness of the photosensitive layer is *ca.* 80–100 nm, measured using an Ambios Tech. XP-2 profilometer. The effective area of one cell is 4 mm². The current–voltage (J–V) measurement of the devices was conducted using a computer-controlled Keithley 236 Source Measure Unit. A xenon lamp with AM 1.5G filter was used as the white light source, and the optical power at the sample was around 100 mW cm⁻².

Synthesis of IDT(BTTh₂)₂

4-Bromo-7-(5′-hexyl-[2,2′-bithiophen]-5-yl)benzo[c][2,1,3]thiadiazole.
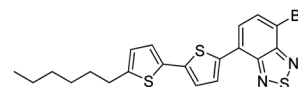
Compound (5′-hexyl-2,2′-bithiophen-5-yl)trimethylstannane (1.3 g, 3 mmol),[38] 4,7-dibromobenzo[c][2,1,3]thiadiazole (3.5 g, 12 mmol), and toluene (50 ml) were added into a 100 ml double-necked round-bottomed flask. The reaction container was de-aerated with argon for 5 min followed by the addition of Pd(PPh₃)₄ (70 mg, 0.06 mmol) and de-aeration for another 20 min with argon to remove O₂. After being heated to reflux for 16 h at 110 °C, the reaction mixture was cooled down to the room temperature, then poured into water and extracted with CH₂Cl₂. Solvent was removed by rotary evaporation and the crude product was purified by flash column chromatography on silica gel using a mixture of dichloromethane and petroleum
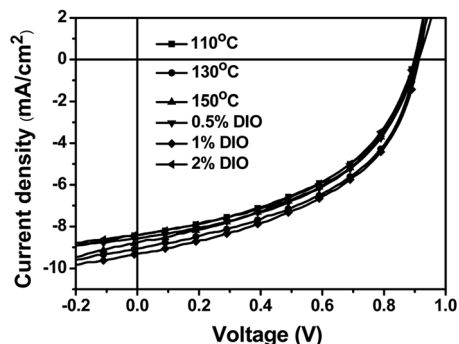
Fig. 5 J–V curves of the SM BHJ solar cells based on IDT(BTTh$_2$)$_2$:PC$_{71}$BM (1 : 3, w/w) under different processing conditions, under the illumination of AM 1.5G at 100 mW cm^{-2}.

ether (1 : 5) as eluant. Finally, compound **5** (0.42 g, 30%) was collected as an orange solid. ^{1}H NMR (400 MHz, CDCl$_3$): δ(ppm) 8.01 (d, 1H), 785 (d, 1H), 7.69 (d, 1H), 7.18 (d, 1H), 7.10 (d, 1H), 6.72 (d, 1H), 2.83–2.79 (m, 2H), 1.73–1.66 (m, 2H), 1.41–1.36 (m 2H), 1.33–1.30 (m 4H), 0.91–0.88 (m 3H).

Synthesis of IDT(BTTh$_2$)$_2$

4-Bromo-7-(5′-hexyl-[2,2′-bithiophen]-5-yl)benzo[c][2,1,3]thiadiazole (**5**) (0.42 g, 0.9 mmol), IDT monomer (**6**) (0.37 g, 0.3 mmol),[37] toluene (15 ml) and DMF (1 ml) were all added into a 100 ml double-necked round-bottomed flask. The reaction container was de-aerated with argon for 5 min followed by the addition of Pd(PPh$_3$)$_4$ (10 mg, 0.009 mmol) and de-aeration for another 20 min with argon to remove O$_2$. After being heated to reflux for 16 h at 110 °C, the reaction mixture was cooled down to room temperature, poured into water and extracted with CH$_2$Cl$_2$. Solvent was removed by rotary evaporation, and the crude product was purified by flash column chromatography on

silica gel using a mixture of dichloromethane and petroleum ether (1 : 5) as eluant. Finally, evaporation of the solvent afforded compound IDT(BTTh$_2$)$_2$ (**6**) (0.3 g, 60%) as a purple power. ^{1}H NMR (400 MHz, CDCl$_3$): δ(ppm) 8.05 (s, 2H), 8.00 (d, 2H), 7.76 (m, 4H), 7.56 (s, 2H), 7.30–7.26 (m, 8H), 7.17 (d, 2H), 7.12–7.09 (m, 10H), 7.72 (d, 2H), 2.83–2.79 (m, 4H), 2.60–2.56 (m, 8H), 1.72–1.66 (m, 4H), 1.63–1.56 (m, 8H), 1.42–1.28 (m, 36H), 0.91–0.87 (m, 18H). Anal. calcd for C$_{104}$H$_{110}$N$_4$S$_6$ (%): C, 73.34%; H, 6.70%; N, 3.31%. Found: C, 73.16%; H, 6.71%; N, 3.36%.

Results and discussion

Synthesis and thermal stability

The general synthetic route for IDT(BTTh$_2$)$_2$ is described in Scheme 1. The important intermediate, 4-bromo-7-(5′-hexyl-[2,2′-bithiophen]-5-yl)benzo[c][2,1,3]thiadiazole, was prepared by a method similar to that reported in the literature.[38] The IDT unit was synthesized according to the published literature.[37] IDT(BTTh$_2$)$_2$ was synthesized using the palladium-catalyzed Stille coupling reaction and exhibited good solubility in common organic solvents such as dichloromethane, chloroform, toluene, chlorobenzene, o-dichlorobenzene, etc.

The thermal stability of IDT(BTTh$_2$)$_2$ was investigated by thermogravimetric analysis (TGA) as shown as in Fig. 1. Under air atmosphere, the onset temperature with 5% weight-loss (T$_d$) of IDT(BTTh$_2$)$_2$ is at over 430 °C, which indicates that the thermal stability of this molecule is adequate for application in optoelectronic devices.

Optical and electrochemical properties

Fig. 2a shows the Ultraviolet-Visible (UV-Vis) absorption spectra of IDT(BTTh$_2$)$_2$ in a dilute o-DCB solution and as a film. The absorption spectra show two peaks from 350 to 700 nm in both solution and film: the first peak at around 400 nm could be
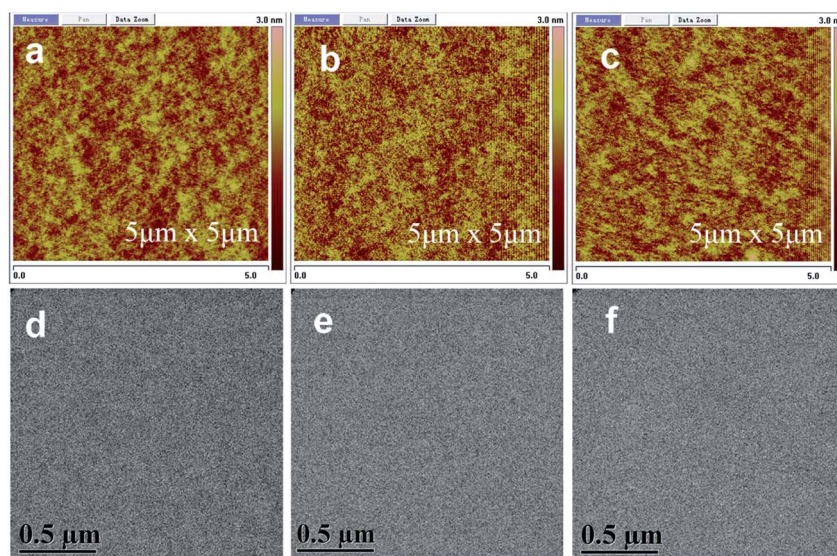

Fig. 6 AFM and TEM images for the IDT(BTTh$_2$)$_2$:PC$_{71}$BM (1 : 3, w/w) blend film: without any treatment (a and d), with 2% DIO as additive (b and e) and thermal annealing at 130 °C for 10 min (c and f).

This journal is © The Royal Society of Chemistry 2013

J. Mater. Chem. A, 2013, 1, 14214–14220 | **14217**

Table 2 Photovoltaic performances of the devices based on IDT(BTTh$_2$)$_2$:PC$_{71}$BM (1 : 3, w/w) under different processing conditions

DIO (vol. %)	Thermal annealing (°C)	V_{oc} (V)	J_{sc} (mA cm^{-2})	FF (%)	PCE (%)
1	—	0.90	8.42	46.7	3.53
2	—	0.91	9.07	47.7	3.92
3	—	0.91	8.78	45.8	3.64
—	110, 10 min	0.91	8.58	47.1	3.68
—	130, 10 min	0.91	9.31	47.3	4.02
—	150, 10 min	0.90	8.41	46.7	3.55

attributed to the localized π–π^* transition of the molecule backbone, whereas the second peak around 600 nm should be ascribed to the strong intermolecular charge transfer (ICT) interaction between the IDT donor unit and BT acceptor units.[39] The absorption spectrum of IDT(BTTh$_2$)$_2$ as a film exhibits an absorption maximum at 610 nm, which is red-shifted by $\sim$25 nm in comparison with that in solution, indicating strong intermolecular interaction in the solid state. The absorption edge (λ_{edge}) of the film is 690 nm from which the optical band gap (E_g^{opt}) of IDT(BTTh$_2$)$_2$ is calculated to be *ca.* 1.80 eV according to $E_g^{opt} = 1240/\lambda_{edge}$.

Electrochemical cyclic voltammetry (CV) was performed to measure the molecular energy levels of IDT(BTTh$_2$)$_2$. The cyclic voltammogram of the IDT(BTTh$_2$)$_2$ film was tested on a glassy carbon disk in 0.1 mol L^{-1} Bu$_4$NPF$_6$ acetonitrile solution. As shown in Fig. 2b, the onset oxidation potentials and the onset reduction potentials were 0.50 V and -1.13 V *vs.* Ag/Ag$^+$, respectively. From the onset potentials of oxidation (φ_{ox}) and reduction (φ_{red}), the HOMO and LUMO energy levels as well as the energy gap (E_g^{EC}) of IDT(BTTh$_2$)$_2$ were calculated, by assuming the energy level of ferrocene/ferrocenium (Fc/Fc$^+$) to be -4.8 eV below the vacuum level.[40] The formal potential of Fc/Fc$^+$ was measured as 0.09 V against Ag/Ag$^+$. According to the equations,

$$\text{HOMO} = -e(\varphi_{ox} + 4.71) \quad \text{(eV)};$$

$$\text{LUMO} = -e(\varphi_{red} + 4.71) \quad \text{(eV)};$$

$$E_g^{EC} = e(\varphi_{ox} - \varphi_{red}) \quad \text{(eV)}$$

where the units of φ_{ox} and φ_{red} are V *vs.* Ag/Ag$^+$.

The HOMO energy level of IDT(BTTh$_2$)$_2$ is -5.21 eV and the LUMO energy level is -3.58 eV. Meanwhile, the electrochemical band gap (E_g^{EC}) is 1.63 eV. The HOMO energy level is lower than those of some small molecules based on benzodithiophene (BDT),[8,11,14] dithienosilole (DTS),[7,9,10,28] triphenylamine (TPA),[41–43] oligothiophene[5,6,22,24,44–46] as well as diketopyrrolopyrrole (DPP)[26,47,48] units. The relatively deep HOMO level implies that the small molecule could be more stable against oxidization, which will enhance the device stability, and also will provide a higher V_{oc} for the SM BHJ solar cells based on IDT(BTTh$_2$)$_2$.[49,50]

Quantum chemistry calculations

Quantum chemistry calculations were performed to demonstrate the electronic structures and molecular energy levels of IDT(BTTh$_2$)$_2$ by using density functional theory (DFT) on the

B3LYP/6-31G(d,p) level.[51] As the side-chain substituents have little influence on the oxidative and reductive properties of the molecule, the six hexyl side chains were all truncated to methyl groups. The optimized molecular geometry, HOMO and LUMO orbital surfaces of IDT(BTTh$_2$)$_2$ are shown in Fig. 3. The backbone of IDT(BTTh$_2$)$_2$ exhibits good planarity and symmetry beneficial for the π–π stacking and hence the high hole mobility. The electron density in the HOMO wave function is delocalized over the whole molecular backbone, whereas the LUMO electron density is mainly localized on the two BT units.

Photovoltaic properties

In order to investigate the photovoltaic properties of IDT(BTTh$_2$)$_2$, SM BHJ solar cell devices were fabricated and characterized with a structure of ITO/PEDOT:PSS/IDT(BTTh$_2$)$_2$:PC$_{71}$BM/Ca/Al. Different D/A weight ratios, such as 1 : 1, 1 : 2, 1 : 2.5, 1 : 3, 1 : 3.5 and 1 : 4 have been scanned to optimized the device performance. Fig. 4a shows *J–V* curves of the solar cells based on IDT(BTTh$_2$)$_2$ under the illumination of AM 1.5G at 100 mW cm^{-2} and the corresponding V_{oc}, J_{sc}, FF, and PCE values of the devices are summarized in Table 1. The best performance was obtained at a weight ratio of 1 : 3, and a PCE of 4.25% with a V_{oc} of 0.93 V, a J_{sc} of 9.42 mA cm^{-2} and a FF of 48.5% was recorded. Fig. 4b shows the external quantum efficiency (EQE) curve of the device with the optimal photovoltaic performance. It can be seen that EQE curve covers a broad response from 300 to 700 nm and exhibits the maximum of 58% at 505 nm. The integrated current density values deduced from the EQE curves and the standard solar spectrum (AM 1.5G) is $\sim$9.0 mA cm^{-2} which agrees well with those obtained from the *J–V* measurement; *i.e.* the variations between the integrated values and the measured values are below 5%.

In order to further improve the performance of the devices, two methods of thermal annealing and the use of 1,8-diiodooctane (DIO) as a solvent additive were applied and investigated. The *J–V* curves of the solar cells based on IDT(BTTh$_2$)$_2$:PC$_{71}$BM (1 : 3, w/w) under the different processing conditions are shown in Fig. 5 and the corresponding photovoltaic parameters are summarized in Table 2. Upon using different contents of DIO as additive, the device based on the blend film processed with the use of 2% DIO exhibits the optimal performance with a PCE of 3.92%, which is still lower than that of the devices processed without DIO. For the devices based on the blend films with thermal annealing under different temperatures, the best performance was obtained under thermal

14218 | *J. Mater. Chem. A*, 2013, **1**, 14214–14220

This journal is © The Royal Society of Chemistry 2013

annealing at 130 °C with a PCE of 4.02%, which is also lower than that of the devices processed without annealing. The results demonstrate that both thermal annealing and the addition of DIO as an additive are of no use in improving the photovoltaic performance. In addition, the morphology of the blend films with or without different treatment methods was investigated using an atomic force microscope (AFM) and transmission electron microscope (TEM) as shown as Fig. 6. All the blend films exhibit a smooth surface morphology with a roughness of ca. 0.3 nm.

Conclusion

In this work, we designed and synthesized a new A–D–A small molecule, IDT(BTTh$_2$)$_2$, based on the indacenodithiophene (IDT) unit as core and benzothiadiazole as an acceptor unit. The small molecule exhibited good solubility in common solvents and thermal stability with the T_d at over 430 °C. The backbone of IDT(BTTh$_2$)$_2$ showed good planarity and symmetry calculated using density functional theory (DFT) at the B3LYP/6-31G level. IDT(BTTh$_2$)$_2$ exhibit a broad absorption in the visible range and a deeper HOMO energy level of −5.21 eV. The devices based on the blend of IDT(BTTh$_2$)$_2$/PC$_{71}$BM (1 : 3 w/w) without any treatment showed the best performance with a PCE of 4.25%, a high V_{oc} of 0.93 V, a J_{sc} of 9.42 mA cm^{-2} and a FF of 48.5%, under the illumination of AM 1.5G at 100 mW cm^{-2}. These results indicated that small molecules based on the indacenodithiophene (IDT) unit are promising materials for use in organic solar cells.

Acknowledgements

References

1 Y. Lin, Y. Li and X. Zhan, Chem. Soc. Rev., 2012, 41, 4245–4272.

2 A. Mishra and P. Baeuerle, Angew. Chem., Int. Ed., 2012, 51, 2020–2067.

3 B. Walker, C. Kim and T.-Q. Nguyen, Chem. Mater., 2011, 23, 470–482.

4 R. Fitzner, E. Mena-Osteritz, A. Mishra, G. Schulz, E. Reinold, M. Weil, C. Koerner, H. Ziehlke, C. Elschner, K. Leo, M. Riede, M. Pfeiffer, C. Uhrich and P. Baeuerle, J. Am. Chem. Soc., 2012, 134, 11064–11067.

5 G. He, Z. Li, X. Wan, Y. Liu, J. Zhou, G. Long, M. Zhang and Y. Chen, J. Mater. Chem., 2012, 22, 9173–9180.

6 Z. Li, G. He, X. Wan, Y. Liu, J. Zhou, G. Long, Y. Zuo, M. Zhang and Y. Chen, Adv. Energy Mater., 2012, 2, 74–77.

7 X. Liu, Y. Su, L. A. Perez, W. Wen, M. F. Toney, A. J. Heeger and G. C. Bazan, J. Am. Chem. Soc., 2012, 134, 20609–20612.

8 Y. Liu, X. Wan, F. Wang, J. Zhou, G. Long, J. Tian and Y. Chen, Adv. Mater., 2011, 23, 5387–5391.

9 Y. Sun, G. C. Welch, W. L. Leong, C. J. Takacs, G. C. Bazan and A. J. Heeger, Nat. Mater., 2012, 11, 44–48.

10 T. S. van der Poll, J. A. Love, N. Thuc-Quyen and G. C. Bazan, Adv. Mater., 2012, 24, 3646–3649.

11 J. Zhou, X. Wan, Y. Liu, Y. Zuo, Z. Li, G. He, G. Long, W. Ni, C. Li, X. Su and Y. Chen, J. Am. Chem. Soc., 2012, 134, 16345–16351.

12 Y.-H. Chen, L.-Y. Lin, C.-W. Lu, F. Lin, Z.-Y. Huang, H.-W. Lin, P.-H. Wang, Y.-H. Liu, K.-T. Wong, J. Wen, D. J. Miller and S. B. Darling, J. Am. Chem. Soc., 2012, 134, 13616–13623.

13 V. Steinmann, N. M. Kronenberg, M. R. Lenze, S. M. Graf, D. Hertel, K. Meerholz, H. Buerckstuemmer, E. V. Tulyakova and F. Wuerthner, Adv. Energy Mater., 2011, 1, 888–893.

14 J. Y. Zhou, Y. Zuo, X. J. Wan, G. K. Long, Q. Zhang, W. Ni, Y. S. Liu, Z. Li, G. R. He, C. X. Li, B. Kan, M. M. Li and Y. S. Chen, J. Am. Chem. Soc., 2013, 135, 8484–8487.

15 L. Huo, S. Zhang, X. Guo, F. Xu, Y. Li and J. Hou, Angew. Chem., Int. Ed., 2011, 50, 9697–9702.

16 H.-Y. Chen, J. Hou, S. Zhang, Y. Liang, G. Yang, Y. Yang, L. Yu, Y. Wu and G. Li, Nat. Photonics, 2009, 3, 649–653.

17 H. Zhou, L. Yang, A. C. Stuart, S. C. Price, S. Liu and W. You, Angew. Chem., Int. Ed., 2011, 50, 2995–2998.

18 S. C. Price, A. C. Stuart, L. Yang, H. Zhou and W. You, J. Am. Chem. Soc., 2011, 133, 4625–4631.

19 T.-Y. Chu, J. Lu, S. Beaupre, Y. Zhang, J.-R. Pouliot, S. Wakim, J. Zhou, M. Leclerc, Z. Li, J. Ding and Y. Tao, J. Am. Chem. Soc., 2011, 133, 4250–4253.

20 Z. He, C. Zhong, X. Huang, W.-Y. Wong, H. Wu, L. Chen, S. Su and Y. Cao, Adv. Mater., 2011, 23, 4636–4643.

21 L. Dou, J. You, J. Yang, C.-C. Chen, Y. He, S. Murase, T. Moriarty, K. Emery, G. Li and Y. Yang, Nat. Photonics, 2012, 6, 180–185.

22 G. He, Z. Li, X. Wan, J. Zhou, G. Long, S. Zhang, M. Zhang and Y. Chen, J. Mater. Chem. A, 2013, 1, 1801–1809.

23 L. Y. Lin, C. W. Lu, W. C. Huang, Y. H. Chen, H. W. Lin and K. T. Wong, Org. Lett., 2011, 13, 4962–4965.

24 Y. Liu, X. Wan, F. Wang, J. Zhou, G. Long, J. Tian, J. You, Y. Yang and Y. Chen, Adv. Energy Mater., 2011, 1, 771–775.

25 M. Singh, R. Kurchania, J. A. Mikroyannidis, S. S. Sharma and G. D. Sharma, J. Mater. Chem. A, 2013, 1, 2297–2306.

26 L. Zhang, S. H. Zeng, L. X. Yin, C. Y. Ji, K. C. Li, Y. Q. Li and Y. Wang, New J. Chem., 2013, 37, 632–639.

27 L. H. Zhang, K. Pei, H. B. Zhao, S. J. Wu, Y. Wang and J. W. Gao, Chem. Phys. Lett., 2012, 543, 199–204.

28 J. Zhou, X. Wan, Y. Liu, G. Long, F. Wang, Z. Li, Y. Zuo, C. Li and Y. Chen, Chem. Mater., 2011, 23, 4666–4668.

29 Y. Zhang, J. Zou, H.-L. Yip, K.-S. Chen, D. F. Zeigler, Y. Sun and A. K. Y. Jen, Chem. Mater., 2011, 23, 2289–2291.

30 M. Zhang, X. Guo, X. Wang, H. Wang and Y. Li, Chem. Mater., 2011, 23, 4264–4270.

This journal is © The Royal Society of Chemistry 2013

J. Mater. Chem. A, 2013, 1, 14214–14220 | 14219

31 X. Wang, H. Luo, Y. Sun, M. Zhang, X. Li, G. Yu, Y. Liu, Y. Li and H. Wang, *J. Polym. Sci., Part A: Polym. Chem.*, 2012, **50**, 371–377.

32 Y. Sun, S.-C. Chien, H.-L. Yip, Y. Zhang, K.-S. Chen, D. F. Zeigler, F.-C. Chen, B. Lin and A. K. Y. Jen, *J. Mater. Chem.*, 2011, **21**, 13247–13255.

33 B. C. Schroeder, Z. Huang, R. S. Ashraf, J. Smith, P. D'Angelo, S. E. Watkins, T. D. Anthopoulos, J. R. Durrant and I. McCulloch, *Adv. Funct. Mater.*, 2012, **22**, 1663–1670.

34 I. McCulloch, R. S. Ashraf, L. Biniek, H. Bronstein, C. Combe, J. E. Donaghey, D. I. James, C. B. Nielsen, B. C. Schroeder and W. Zhang, *Acc. Chem. Res.*, 2012, **45**, 714–722.

35 K.-S. Chen, Y. Zhang, H.-L. Yip, Y. Sun, J. A. Davies, C. Ting, C.-P. Chen and A. K. Y. Jen, *Org. Electron.*, 2011, **12**, 794–801.

36 H. Bronstein, R. S. Ashraf, Y. Kim, A. J. P. White, T. Anthopoulos, K. Song, D. James, W. Zhang and I. McCulloch, *Macromol. Rapid Commun.*, 2011, **32**, 1664–1668.

37 X. Guo, M. Zhang, J. Tan, S. Zhang, L. Huo, W. Hu, Y. Li and J. Hou, *Adv. Mater.*, 2012, **24**, 6536–6541.

38 R. C. Coffin, J. Peet, J. Rogers and G. C. Bazan, *Nat. Chem.*, 2009, **1**, 657–661.

39 X. Guo, M. Zhang, L. Huo, C. Cui, Y. Wu, J. Hou and Y. Li, *Macromolecules*, 2012, **45**, 6930–6937.

40 Q. Sun, H. Wang, C. Yang and Y. Li, *J. Mater. Chem.*, 2003, **13**, 800–806.

41 J. Kim, H. M. Ko, N. Cho, S. Paek, J. K. Lee and J. Ko, *RSC Adv.*, 2012, **2**, 2692–2695.

42 J. Y. Pan, L. J. Zuo, X. L. Hu, W. F. Fu, M. R. Chen, L. Fu, X. Gu, H. Q. Shi, M. M. Shi, H. Y. Li and H. Z. Chen, *ACS Appl. Mater. Interfaces*, 2013, **5**, 972–980.

43 A. L. Tang, L. J. Li, Z. H. Lu, J. H. Huang, H. Jia, C. L. Zhan, Z. A. Tan, Y. F. Li and J. N. Yao, *J. Mater. Chem. A*, 2013, **1**, 5747–5757.

44 Y. S. Liu, X. J. Wan, B. Yin, J. Y. Zhou, G. K. Long, S. G. Yin and Y. S. Chen, *J. Mater. Chem.*, 2010, **20**, 2464–2468.

45 J. K. Lee, B. S. Jeong, J. Kim, C. Kim and J. Ko, *J. Photochem. Photobiol., A*, 2013, **251**, 25–32.

46 B. Yin, L. Y. Yang, Y. S. Liu, Y. S. Chen, Q. J. Qi, F. L. Zhang and S. G. Yin, *Appl. Phys. Lett.*, 2010, **97**, 023303.

47 Y. Zhang, J. H. Liu and T. Q. Nguyen, *ACS Appl. Mater. Interfaces*, 2013, **5**, 2347–2353.

48 S. Y. Qu and H. Tian, *Chem. Commun.*, 2012, **48**, 3039–3051.

49 M. C. Scharber, D. Wuhlbacher, M. Koppe, P. Denk, C. Waldauf, A. J. Heeger and C. L. Brabec, *Adv. Mater.*, 2006, **18**, 789–794.

50 G. Dennler, M. C. Scharber and C. J. Brabec, *Adv. Mater.*, 2009, **21**, 1323–1338.

51 R. G. Parr and Y. Weitao, *Density Functional Theory of Atoms and Molecules*, Oxford University Press, New York, 1989.